OPEN ACCESS
ARTICLE

Efficient, Green Non-aqueous Microwave-assisted Synthesis of Anatase TiO_2 and Pt Loaded TiO_2 Nanorods with High Photocatalytic Performance

Regular Paper

Emanuela Filippo[1]*, Agostina Lina Capodilupo[2], Claudia Carlucci[3], Patrizia Perulli[1], Francesca Conciauro[2], Giuseppina Anna Corrente[2], Barbara Federica Scremin[2], Giuseppe Gigli[2,4,5] and Giuseppe Ciccarella[1,2]*

1 Department of Innovation Engineering, University of Salento, Lecce, Italy
2 CNR NANOTEC - Institute of Nanotechnology of the National Research Council, c/o Campus Ecotekne, University of Salento, Lecce, Italy
3 Department of Chemistry, University of Bari, Bari, Italy
4 Center for Biomolecular Nanotechnologies (CBN) of Italian Institute of Technology (IIT), Arnesano (LE), Italy
5 Department of Physics, University of Salento, Lecce, Italy
*Corresponding author(s) E-mail: emanuela.filippo@unisalento.it; giuseppe.ciccarella@unisalento.it

Received 11 March 2015; Accepted 02 July 2015

DOI: 10.5772/61147

Abstract

A high-yield synthesis of pure anatase titania nanorods has been achieved through a nonaqueous microwave-based approach. The residual organics on nanoparticles surfaces were completely removed under ozone flow at room temperature in air. The TiO_2 nanorods, with average lengths of 27.6 ± 5.8 nm and average diameters of 3.2 ± 0.4 nm, were characterized by powder X-Ray diffraction, transmission electron microscopy, selected area diffraction, BET surface area analysis and FT-IR spectroscopy. The photocatalytic performances of the as-synthesized TiO_2 nanorods and platinum loaded TiO_2 nanorods were implemented with respect to both commercial P25 and platinum loaded P25. Performance enhancements should be attributed to effects like differences in the adsorption capacity and in the separation efficiency of the photogenerated electrons-holes.

Keywords Anatase, Pt, Nanorods, Microwave, Photocatalysis

1. Introduction

One-dimensional (1-D) nanostructured materials, including nanorods and nanowires, have received significant attention. This is due to properties that are derived from low size, quantum confinement effects and their potential applications including interconnects and functional blocks in nanoscale devices [1]. Nanosized titania is intensively

studied for the chemical and physical properties, which are of interest for applications in gas sensing [2], catalysis [3], photocatalysis [4-6], pigments [7], optics [8] and photovoltaic cells [9]. In TiO_2-based photocatalysts, the photogenerated electrons (e^-) and holes (h^+) migrate to the nanocrystal surface. Here, they act as redox sources, ultimately leading to the destruction of pollutants. The photocatalytic activity of TiO_2 depends on the crystal structure, morphology, particle size, surface area and porosity - properties that vary with the preparation methods [10]. Numerous studies report on the synthesis of different morphologies TiO_2 nanostructures with sol-gel and hydrothermal techniques. These typically need high pressures and temperatures, long duration and complex procedures [11]. Seeking simple, fast and relatively low temperature methods without calcinations steps is still of interest [12]. Recently, microwave irradiation has been reported to effectively enhance the efficiency of preparation methods of inorganic nanomaterials [13-16]. Advantages include the obtainable molecular homogeneity and rapid heating. In higher yields, this leads to a reduction in the reaction time. A further advantage is product uniformity, which results in better final properties. Thus, microwave methods allow very short time reactions for the synthesis of organic and inorganic materials, although this is still less explored for inorganic materials [17]. In this paper, we report a nonaqueous microwave-assisted sol-gel method for the preparation of high purity anatase TiO_2 nanorods with a temperature of 210 °C and a reaction time of 45 min, using Ti (IV) isopropoxide as a precursor, benzyl alcohol as a solvent and oleic acid as an additive reagent. The physicochemical characteristics of nanorods in terms of morphology, crystallization and surface area were characterized by X-ray diffraction (XRD), transmission electron microscopy (TEM), selected area diffraction pattern (SAD), FT-IR spectroscopy and BET surface area analysis. The anatase TiO_2 nanorods and the Pt loaded TiO_2 nanorods were ozone-treated for surfactants removal before the photocatalytic tests. The degradation of rhodamine B (RhB) in aqueous solution under simulated solar light was experimented with the synthesized nanorods and compared with commercial P25 and platinum loaded P25 nanoparticles. The results of the RhB degradation significantly improved with the synthesized nanocrystals.

2. Materials and Methods

Titanium (IV) isopropoxide TTIP, benzyl alcohol, oleic acid, chloroplatinic acid solution 8 wt. % in H_2O, Rhodamine B (MW: 479.02 g/mol, purity 99%), TiO_2 Degussa P-25 (80% anatase, 20% rutile) were purchased from Sigma Aldrich (USA). All of the chemicals and solvents were of analytical grade and used without further purification. Double distilled water was filtered through a Millipore membrane filter before being used in the experiments.

2.1 Synthesis of TiO2 Nanorods

As a typical synthesis procedure, 1ml of TTIP (3 mmol) was slowly added into 10 ml of benzyl alcohol in a Teflon vessel. Then, oleic acid (27 mmol) was added dropwise under vigorous magnetic stirring. The vessel was sealed and exposed to 2.45 GHz microwave irradiation using a microwave digestion system (model Mars, CEM, Matthews, NC). The reaction mixture was maintained at 210 °C for 45 min under medium stirring. The resulting product was collected and washed several times with methanol and finally dried under vacuum at 40 °C.

2.2. Removal of the Capping Layer from the TiO_2 Nanocrystals

The nanostructures obtained by sol-gel and hydrothermal procedures are usually capped by organic molecules and cannot be directly applied as catalysts. Several strategies, including thermal and chemical treatments, have been commonly used for the removal of the capping agents. A series of spectroscopic investigations [18-20] demonstrated that thermal treatments were able to remove capping agents, but organic portions were transformed into a thermally stable form of carbon. Moreover, high-temperature oxidation and reduction treatments can lead to particle growth and monodispersity loss.

In the present work, the oleic acid that coordinated on the TiO_2 nanorods surface was removed through ozone (O_3) treatment in air and at room temperature. Dried TiO_2 samples (200 mg) were placed in a cylindrical neck spherical glass container and treated with an ozone flow for 1 h, under vigorous stirring. The ozone oxidation process transformed the carbon, which contained compounds, into carbon dioxide and water [21].

2.3. Preparation of the Pt Loaded TiO_2 Nanorods

The photo-deposition of the Pt nanoparticles was performed on commercial P25 and on the synthesized TiO_2 sample after O_3 treatment. As a typical procedure, in a 100 ml beaker, TiO_2 (2.0 gr) was dispersed in 50 ml of methanol. H_2PtCl_6 (0.50 ml, 8 wt% aqueous solution) was added. The reaction mixtures were then irradiated with a 150 W Xe lamp (without optical filters) for 30 min. The milky white suspensions turned to a greyish colour with Pt deposition. The resultant Pt-TiO_2 composites were retrieved by 3700 rpm centrifugation, washed five times with excess methanol and dried under vacuum.

2.4 Characterization of Nanocrystals

The samples were characterized by X-ray diffraction (XRD), transmission electron microscopy (TEM), selected area diffraction pattern (SAD), BET surface area analysis, FT-IR spectroscopy and coupled plasma atomic emission spectroscopy (ICP-AES).

X-ray diffraction measurements were carried out in the reflection mode on a Rigaku diffractometer with Cu Kα radiation (λ = 0.154 nm). The X-ray diffraction data were collected at a scanning rate of 0.02°/s in 2θ from 20° to 70°. TEM observations were taken using a Jeol Jem 1011 transmission electron microscope, operated at 100 kV. The specimens for the TEM analysis were prepared by drop

casting a single drop of the sample in ethanol solution onto standard carbon supported 300-mesh copper grids and dried slowly in air. The nitrogen adsorption–desorption isotherms at 77 K were obtained using Brunauer–Emmett–Teller (BET) characterization setup and recorded using a Quantachrome ASiQwin system. ICP-AES was performed with a Varian Vista AX ICP-AES instrument. The FT-IR spectra of the TiO_2 nanorods were collected using a Jasco FT/IR-6300 spectrometer with a resolution of 0.07 cm^{-1}. A UV-visible absorption spectroscopy was performed using a Varian Cary 300 Scan spectrophotometer with a 10-mm path length quartz cuvette.

2.5 Photodegradation of Rhodamine B

The photocatalytic degradation of Rhodamine B was investigated with P25, TiO_2, Pt-P25 and Pt-TiO_2 catalysts. The photodegradation of Rhodamine B (RhB) for the different samples was tested using a 150 W Xe lamp (LOT Oriel Gmbh) as an artificial sunlight source.

The titania catalysts (50 mg) were sonicated in 10 ml distilled water (15 min) to ensure their complete solution dispersion. The catalysts were then mixed with a RhB 10^{-5} M in distilled water (50 ml) solution and kept in the dark for 30 min to reach an adsorption/desorption equilibrium. The mixtures were continuously stirred in air and irradiated by the Xe lamp, which was equipped with a 420 nm cutoff filter for UV radiation removal. The distance between the lamp and the bottom of the solution was about 10 cm. The progress of the reactions was monitored by recording the irradiated samples absorption spectra every 5 min.

3. Results and Discussion

3.1 Characterization of the Samples

The representative X-ray diffraction patterns of the obtained TiO_2 sample are shown in Figure 1 a.

All of the observed peaks were assigned to a tetragonal TiO_2 anatase with lattice constants a = b = 0.37710 nm, c = 0.9430 nm and $\alpha = \beta = \gamma = 90°$, in agreement with the standard diffraction data (JCDS No 21-1272). No other peaks were detected, indicating the high purity of the samples. The XRD pattern of the commercial P25 nanoparticles, which is presented in Figure 1a, confirmed the presence of anatase and rutile phases (JCDS No 21-1276). The XRD spectrum, which was acquired after the Pt photodeposition, did not show any differences with respect to the un-loaded sample. When the impurity level on any sample's surface, Pt in this case, remains less than 5%, it is less likely to be detected by XRD. However, in this study, the presence of Pt on the surface of the TiO_2 nanorods was confirmed by an ICP-AES analysis and quantified at 1 wt%.

The surface characterization of oleic acid capped and ozone-treated nanorods was carried out through FT-IR spectroscopy (Figure 2).

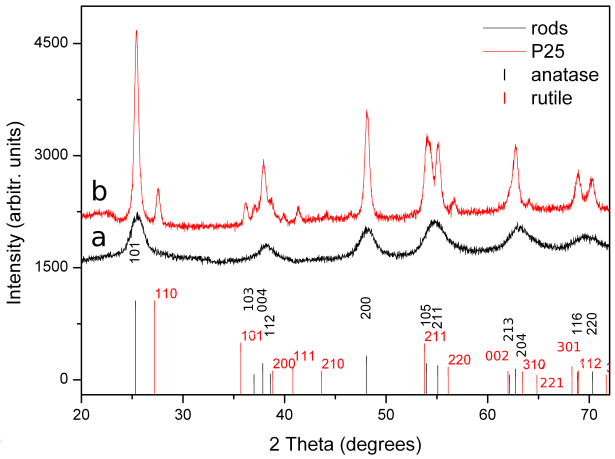

Figure 1. XRD patterns of: a) synthesized TiO_2 nanorods and b) P25 nanoparticles

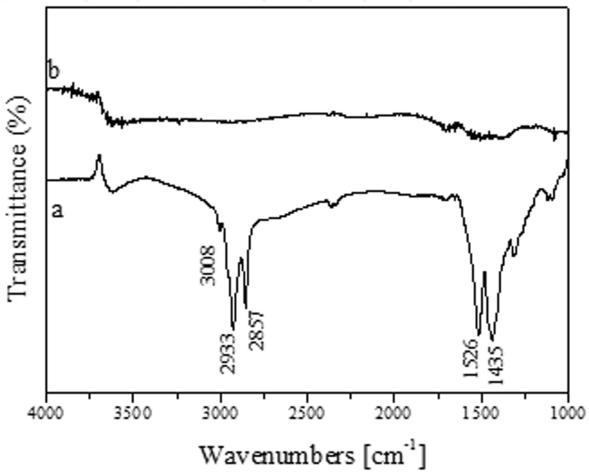

Figure 2. FT-IR spectra of TiO_2 nanorods: a) before and b) after treatment under ozone flow for 1 h

The oleic acid coated nanorods (Figure 2a) exhibited intense antisymmetric and symmetric C-H stretching vibrations (at 2933 and 2857 cm^{-1}, respectively) of the -CH_2- groups in the hydrocarbon moiety. These disappeared with the removal of the oleic acid (Figure 2b) with ozone treatment. The shoulder at 2960 cm^{-1} could be associated with the asymmetric stretching of the terminal -CH_3 group of the alkyl chain [22]. At 3008 cm^{-1}, a weak but definite band was also present, which was caused by the olefinic C-H stretching. This was superimposed on the broad stretching band of O- from the titanol groups of adsorbed H_2O, which was centred at 3300 cm^{-1}.

The antisymmetric and symmetric stretching vibrations of the COO^- carboxylate anions were revealed by the two characteristic bands, which were centred respectively at 1526 and 1435 cm^{-1}. They had a wavenumber difference of ~91 cm^{-1}, which is indicative of a "chelating bidentate" binding mode of carboxylate on the TiO_2 surface [23].

A transmission electron microscopy (TEM) and selected area diffraction pattern (SAD) were employed to investigate the morphology and structure of the prepared TiO_2 nanorods and P25 nanoparticles (Figure 3).

Furthermore, the corresponding SAD pattern, which is reported in Figure 3b, clearly showed that the nanorods were highly crystalline. It exhibited diffraction spotted rings with d spacing, which could be indexed according to tetragonal TiO_2 anatase.

Figure 3a clearly shows that the prepared titania sample consisted of high aspect ratio nanorods with average lengths of 27.6 ± 5.8 nm and average diameters of 3.2 ± 0.4 nm.

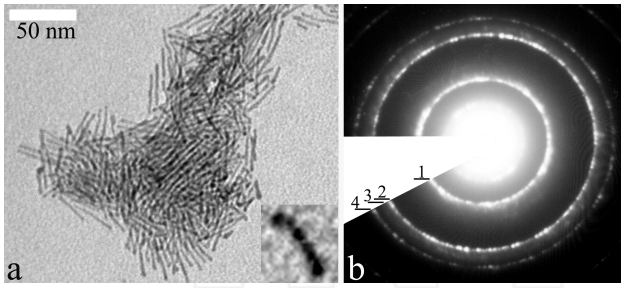

Figure 3. (a) TEM image of the synthesized TiO_2 nanoparticles, with the corresponding (b) selected area diffraction pattern. Inset in (a): high magnification image of a single nanorod.

Table 1 compares the experimental interplanar spacings d values, calculated from the SAD diffraction pattern and literature reported data. These results confirmed the high purity of the obtained products and showed a deviation for the (004) plane, which could be ascribed to the presence of a small distortion in the rod's structure [24].

	hkl	*d (Å) exp.*	*d (Å)* JCDS 21-1271
1	101	3.500	3.516
2	004	2.034	2.379
3	200	1.881	1.892
4	211	1.667	1.666

Table 1. Interplanar spacings d exp. deduced from the SAD pattern of Figure 3b, together with the literature of the corresponding ones (JCSD 21-1271). The italic numbers in the first column represent the labels of reflections in the diffraction pattern, according to Figure 3b.

The TEM observation of the P25 sample confirmed the particles with a relatively uniform particle size distribution, with an average size of about 24.1 ± 9.5 nm, as declared by the producer Sigma Aldrich.

A careful analysis at high magnification on the single nanorods showed that, in some cases, the nanorods were joined up head-to-head by small spherical nanoparticles in a specific direction (inset of Figure 3a).

Previous studies demonstrated the controlled growth of anatase titania nanorods by hydrolysis of TTIP in oleic acid [10]. However, such strategies required a very long reaction time (at least 6 h). In the present case, the titania nanorods were achieved within 45 min under microwave, without further treatment. The use of benzyl alcohol as a solvent was essential, as the microwave-assisted synthesis required a polar solvent to facilitate the heating of the system. We proposed two competitive possible formation mechanisms for the nanorods, as follows. It is well known that oleic acid may serve as a adsorbing-chelating ligand, inhibiting the growth rate along some crystallographic directions [10]. In the TTIP-oleic acid reaction system, in terms of the growth of anisotropic nanoparticles, the most influencing factor in shape control is the rate of water supply. In fact, one-dimensional growth can be achieved by fast hydrolysis of the precursors. Meanwhile, nearly spherical particles are obtained when water is added slowly. In our experimental conditions, thanks to microwave heating, the esterification process was quicker with respect to conventional heating. Consequently, more water was simultaneously released for the benefit of the rod's formation. In such a mechanism, the crystal surface energy played an important role for the shape of the nanocrystals. Due to the high surface energy of {001} face, the spherical nanocrystal generated at the initial reaction stage grow along the (001) direction [25].

However, a careful high magnification TEM analysis of the nanorods demonstrated that, along with preferential growth, another rod mechanism formation could exist: oriented attachment mechanism (inset of Figure 3a).

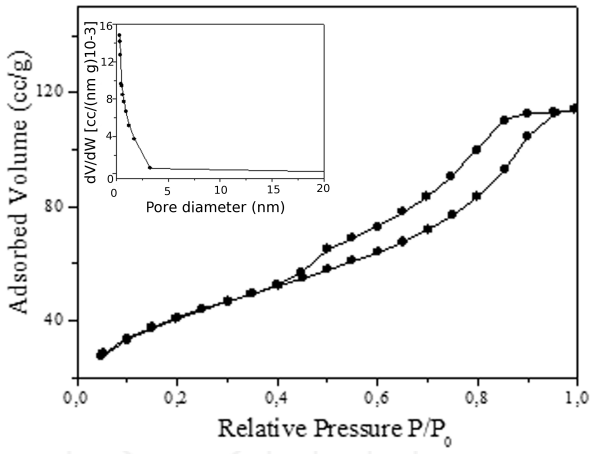

Figure 4. Nitrogen adsorption-desorption and pore size distribution (inset) of the ozone-treated TiO_2 nanorods

The oriented attachment mechanism has been reported for a variety of metal oxide systems and, in particular, for the crystalline anatase TiO_2 nanorods, by the reaction [12] between $TiCl_4$ and benzyl alcohol at 80°C and by the reaction [25] of tetrabutyl titanate (TBT), H_2O and oleic acid at 240°C. It is said that the oriented attachment between spherical nanocrystals reduces the surface energy and can usually be observed in (001) direction because of its high surface energy [12].

The structural and textural properties of the ozone-treated TiO_2 samples were investigated by N_2 adsorption–desorption isotherms at 77 K. Figure 4 shows the obtained results,

which were analysed by the BET method for surface area and BJH pore size distribution in the inset. The sample isotherm was of type IV, which is characteristic of a mesoporous material. The Brunauer–Emmett–Teller (BET) specific surface area analysis resulted in 60.18 $m^2 g^{-1}$ - higher than the reported surface area of P25 nanoparticles (56 $m^2 g^{-1}$). The BJH pore size distributions of the prepared titania nanorods is shown in the inset of Figure 4.

3.2 Photocatalytic Degradation of Rhodamine

As a function of time, the photocatalytic degradation of RhB in aqueous solution was evaluated using ozone treated TiO_2 nanorods and Pt loaded TiO_2 nanorods. The experimental data were compared with those obtained using P25 and Pt-P25 nanoparticles. Blank experiments were carried out on a RhB solution that did not contain the catalyst and proved to have negligible dye degradation upon direct visible irradiation. In addition, the RhB-titania samples that were kept in the dark did not show any appreciable absorbance changes over time. Under the lamp illumination and in the presence of titania, the photodecomposition of the RhB proceeded in both a photocatalytic pathway and a photosensitization pathway. Both of these processes depend on the titania photocatalytic activity, as reflected by the RhB photodegradation [12]. The RhB concentration was determined by the measurements of its maximum absorption at 554 nm (Figure 5).

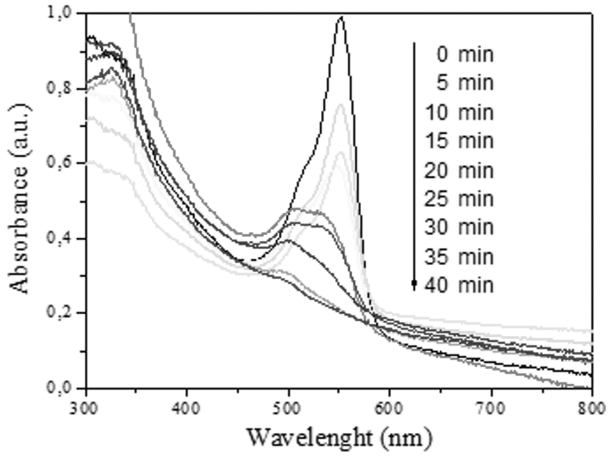

Figure 5. Change in the characteristic absorbance intensity of the RhB solution (at 554 nm) as a function of irradiation time for Pt-TiO_2 nanorods sample

Figure 5 shows the UV-Vis characteristic absorption intensity of the RhB solution decreasing with the irradiation time for a sample of Pt-TiO_2 nanorods. In the photodegradation process, a blue shift of the absorption maximum to 498 nm and an increase in the irradiation time was clearly observed. The hypsochromic shift implied the cleavage of the conjugated structure of RhB [26]. The curves of the RhB relative concentration changes (calculated from the absorption at 554 nm) versus the irradiation time for each sample are shown in Figure 6a. After 60 min of light irradiation, the RhB degradation in the presence of TiO_2 nanorods was up to 90%, while it was significantly higher than 50%. As is shown in Figure 6b, the degradation of RhB followed a pseudo-first-order kinetic. The photodegradation rate constants (k) were 0.043 min^{-1} for TiO_2 nanorods, 0.013 min^{-1} for P25, 0.067 min^{-1} for Pt-TiO_2 nanorods and 0.030 min^{-1} for Pt-P25. Hence, we can conclude that both the anatase TiO_2 nanorods that were synthesized by the microwave-assisted approach possessed higher photocatalytic activity than P25 and Pt-P25.

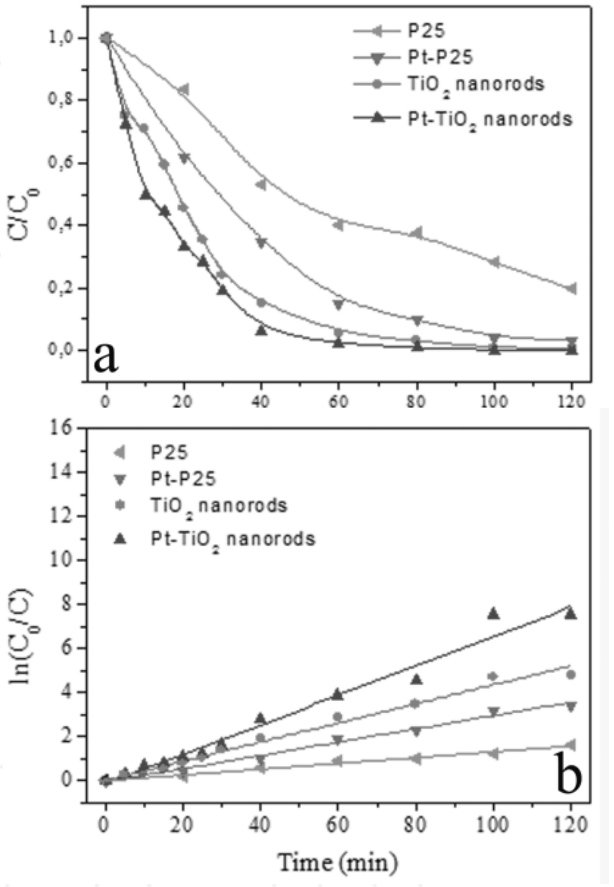

Figure 6. (a) Photocatatalytic degradation of RhB solution by synthesized TiO_2 and Pt-TiO_2 and reference P25 and Pt-P25 samples under visible light irradiation; (b) first order kinetic plot for the photodegradation of RhB

Several reasons may account for the high activity of the anatase TiO_2 nanorods that were prepared in this study. High purity anatase phase, high surface area, small crystal size and cleaned surfaces play important roles in the enhancement of the photocatalytic activities since they guarantee a high density of active sites available for surface reactions, as well as a high interfacial charge carrier transfer rate [12]. Therefore, the BET surface area for P25 was only slightly less than the one for anatase nanorods. Thus, the photocatalytic enhancement should be attributed to other effects like differences in the adsorption capacity and in separation efficiency of photogenerated e-h [28]. The enhancement in the organic pollutants' decomposition rates in the presence of metal loaded TiO_2 nanomaterials

has been previously discussed by several authors [27]. Deposits of platinum and other noble metals enhance the separation of the electron–hole pairs in a semiconductor. Platinum islands are very effective traps for the electrons due to the formation of a Schottky barrier at the metal–semiconductor contact [27]. Improvements in the photocatalytic performances upon platinization were observed for both the nanorods and P25. The mechanism of degradation of RhB by TiO_2 under visible light irradiation has been studied in previous literature [26]. It is resumed in three steps:

$$RhB^{*} + TiO_2 \rightarrow TiO_2\left(e^{-}\right) + RhB^{+\bullet}$$

$$TiO_2\left(e^{-}\right) + O_2 \rightarrow TiO_2 + O_2^{-\bullet}$$

$$RhB^{+\bullet}\left(RhB\right) + O_2^{-\bullet} \rightarrow \text{structure cleavage}$$

In Pt loaded TiO_2, the main enhancing effect is reported [27] to be a higher rate of production of oxidising species, holes or $HO^{\cdot}$ radicals. In the presence of molecular oxygen, the cathodic process is the O_2 reduction by conduction band electrons. This can also result in the formation of hydroxyl radicals, also contributing to the degradation of carboxylic acids:

$$e^{-} + O_2 \rightarrow O_2^{\bullet-}$$

$$O_2^{\bullet-} + 2H^{+} + e^{-} \rightarrow H_2O_2$$

$$H_2O_2 + e^{-} \rightarrow HO^{\bullet} + OH^{-}$$

The anodic process in the case of carboxylic acids can be viewed as the attack by holes or hydroxyl radicals, initially forming a carboxylate radical. This readily decomposes irreversibly liberating CO_2 [27].

$$RCOOH + h^{+}\left(HO\right)ads \rightarrow RCOO^{\bullet} + H^{+}\left(H_2O\right) \rightarrow CO_2 + R^{\bullet}$$

4. Conclusions

In this paper, an environmentally friendly and high-yield microwave-assisted method for the synthesis of TiO_2 nanorods has been presented using Ti (IV) isopropoxide as a precursor, benzyl alcohol as a solvent and oleic acid as an additive reagent. High aspect ratio nanorods with average lengths of 27.6 ± 5.8 nm and average diameters of 3.2 ± 0.4 nm were obtained with a reaction time of 45 min.

The residual organics on the surfaces of the nanoparticles were completely removed using a new low-cost treatment under ozone flow, at room temperature in air. The nanorods were then loaded with Pt. The experimental results demonstrated that the synthesized anatase titania nanorods exhibited higher photocatalytic activity compared to P25 and Pt-P25 and was further increased by Pt loading. Improved performances among the studied samples should be attributed to effects like differences in the adsorption capacity and the separation efficiency of the photogenerated e-h.

5. Acknowledgements

This research was supported by PON 254/Ric. Strengthening of "Research Center for Human and Environmental Health" Cod. PONa3_00334, PON prot. n. 84/Ric. of 2 March 2012 NAnoMAterials for susTAinable construction (NAMASTE) prot. PON04a3_00107- Puglia region grants and supports of the regional partnership for innovation NAno/MIcro STructuring matErials for the construction and other industrial (NAMISTE) Cod. 2Y6DME5.

6. References

[1] Joo J, Kwon S G, Yu T, Cho M, Lee J, Yoon J, Hyeon T (2005) Large Scale Synthesis of TiO_2 Nanorods Via Nonhydrolytic Sol-gel Ester Elimination Reaction and Their Application to Photocatalytic Inactivation of E. Coli. J. Phys. Chem. B 109 15297-15302.

[2] Ferroni M, Carotta M C, Guidi V, Martinelli G, Ronconi F, Sacerdoti M, Traversa E (2001) Preparation and Characterization of Nanosized Titania Sensing Film. Sens. Actuator B: Chem. 77 163-166.

[3] Stark W J, Wegner K, Pratsinis S E, Baiker A (2001) Flame Aerosol Synthesis of Vanadia-titania Nanoparticles: Structural and Catalytic Properties in the Selective Catalytic Reduction of NO by NH_3. J. Catal. 197 182-191.

[4] Wu J M, Qi B (2007) Low Temperature Growth of a Nitrogen Doped Titania Nanoflower Film and Its Ability to Assist Photodegradation of Rhodamine B in Water. J. Phys. Chem. C 666-673.

[5] Carlucci C, Xu H, Scremin B F, Giannini C, Altamura D, Carlino E, Videtta V, Conciauro F, Gigli G, Ciccarella G. (2014) Selective Synthesis of TiO_2 Nanocrystals with Morphology Control with the Microwave-solvothermal Method. Cryst. Eng. Comm 16 1817-1824.

[6] Filippo E, Carlucci C, Capodilupo A L, Perulli P, Conciauro F., Corrente G A, Gigli G, Ciccarella G (2015) Facile Preparation of TiO_2-Polyvinyl Alcohol Hybrid Nanoparticles with Improved Visible Light Photocatalytic Activity. Appl. Surf. Sci. 331 292-298.

[7] Feldmann C (2001) Preparation of Nanoscale Pigment Particles. Adv. Mater. 13 1301-1303.

[8] Frindell K L, Bartl M H, Popitsch A, Stucky G D (2002) Sensitized Luminescence of Trivalent Europium by Three-dimensionally Arranged

Anatase Nanocrystals in Mesostructured Titania Thin Films. Angew. Chem. Int. Ed. 41 959-962.

[9] Loiudice A, Rizzo A, De Marco L, Belviso M R, Caputo G, Cozzoli P D, Gigli G (2012) Organic Photovoltaic Devices with Colloidal TiO_2 Nanorods As Key Functional Components. Phys. Chem. Chem. Phys. 14 3957-3995.

[10] Cozzoli P D, Kornowski A, Weller H (2013) Low Temperature Synthesis of Soluble and Processable Organic-capped Anatase TiO_2 Nanorods. J. Am. Chem. Soc. 125 14539-14548.

[11] Ito S, Murakami T N, Comte P, Liska P, Gratzel C, Nazeeruddin M K, Gratzel M (2008) Fabrication of Thin Film Dye Sensitized Solar Cells with Solar to Electric Power Conversion Efficiency over 10%. Thin Solid Films 516 4613–4619.

[12] Jia H, Zheng Z, Zhao H, Zhang L, Zou Z (2009) Nonaqueous Sol-gel Synthesis and Growth Mechanism of Single Crystalline TiO_2 Nanorods with High Photocatalytic Activity. Materials Research Bulletin 44 1312-1316.

[13] Hart J N, Cervini R, Cheng Y B, Simon G P, Spiccia L (2004) Formation of Anatase TiO_2 by Microwave Processing. Solar Energy Materials and Solar Cells 84 135-143.

[14] Xu H, Carlucci C, Scremin B F, Giannini C, Sibillano T, Scrascia A, Capodilupo A L, Gigli G, Ciccarella G (2014) Synthesis of Ultrafine Anatase Titanium Dioxide (TiO2) Nanocrystals by the Microwave-Solvothermal Method. Journal of Nanoengineering and Nanomanufacturing 4 28 - 32.

[15] Carlucci C, Xu H, Scremin B F, Giannini C, Sibillano T, Carlino E, Videtta V, Gigli G, Ciccarella G (2014) Controllable One-pot Synthesis of Anatase TiO_2 Nanorods with the Microwave-Solvothermal Method. Sci. Adv. Mater. 6 1668 - 1675.

[16] Carlucci C, Scremin B F, Sibillano T, Giannini C, Filippo E, Perulli P, Capodilupo A L, Corrente G A Ciccarella G. (2014) Microwave-Assisted Synthesis of Boron-Modified TiO_2 Nanocrystals. Inorganics 32 264 - 277.

[17] Jia X, He W, Zhang X, Zhao H, Li Z, Feng Y (2007) Microwave Assisted Synthesis of Anatase TiO_2 Nanorods with Mesopores. Nanotechnology 18 075602 1-7.

[18] Borodko Y, Habas S E, Koebel M M, Yang P, Frei H, Somorjai G A (2006) Probing the Interaction of Poly(vinylpyrrolidone) with Platinum Nanocrystals by UV-Raman and FTIR. J. Phys. Chem. B 110 23052–23059

[19] Borodko Y, Lee H S, Joo S H, Zhang Y, Somorjai G A (2010) Spectroscopic Study of the Thermal Degradation of PVP-capped Rh and Pt Nanoparticles in H_2 and O_2 Environments. J. Phys. Chem. C 114 1117–1126

[20] Borodko Y, Humphrey S M, Tilley T D, Frei H, Somorjai G A (2007) Charge–transfer Interaction of Poly(vinylpyrrolidone) with Platinum and Rhodium Nanoparticles. J. Phys. Chem. C 111 6288–6295.

[21] Park J Y, Aliaga C, Renzas J R, Lee H, Somorjai G A (2009) The Role of Organic Capping Layer of Platinum Nanoparticles in Catalytic Activity of CO Oxidation. Catal. Lett. 1 1-6.

[22] Thistlethwaite P J, Hook M S (2000) Diffuse Reflectance Fourier Transform Infrared Study of the Adsorption of Oleate/oleic Acid onto Titania. Langmuir 16 4993-4998.

[23] Nara M, Torii H, Tasumi M (1996) Correlation between the Vibrational Frequencies of the Carboxylate Group and the Types of Its Coordination to a Metal Ion: An Ab Initio Molecular Orbital Study. J. Phys. Chem. 100 19812-19817.

[24] De Caro L, Carlino E, Cozzoli P D, Giannini C (2010) Electron Diffractive Imaging of Oxygen Atoms in Nanocrystals at Sub-angstrom Resolution. Nat. Nanotech. 5 360-365.

[25] Kong W, Liu B, Ye B, Yu Z, Wang H, Qian G, Wang Z (2011) An Experimental Study on the Shape Changes of TiO_2 Nanocrystals Synthesized by Microemulsion-Solvothermal Method, Hindawi Publishing Corporation Journal of Nanomaterials ID 467083 1-6.

[26] Chen C C, Zhao W, Lei P, Zhao J C, Serpone N (2004) Photosensitized Degradation of Dyes in Polyoxometalate Solutions Versus TiO_2 Dispersions Under Visible Light Irradiation: Mechanistic Implications. Chem. Eur. J. 10 1956-1965.

[27] Hufschmidt D, Bahnemann D, Testa J J, Emilio C A, Litter M I (2002) Enhancement of the Photocatalytic Activity of Various TiO_2 Materials by Platinisation. J. Photochem. Photobiol. A: Chem. 148 223-231.

[28] Jin S, Li Y, Xie H, Chen X, Tian T, Zhao X (2012) Highly Selective Photocatalytic and Sensing Properties of 2D-ordered Dome Films of Nano Titania and Nano Ag^{2+} Doped Titania. J. Mater. Chem. 22, 1469-1476.